Applied Catalysis B: Environmental 95 (2010) 137–143

Contents lists available at ScienceDirect

Applied Catalysis B: Environmental

journal homepage: www.elsevier.com/locate/apcatb

Nanoparticle-assembled Co-B thin film for the hydrolysis of ammonia borane: A highly active catalyst for hydrogen production

N. Patel *, R. Fernandes, G. Guella, A. Miotello

Dipartimento di Fisica, Università degli Studi di Trento, Via Sommarive, 14, I-38100 Povo, Trento, Italy

ARTICLE INFO

Article history:
Received 4 November 2009
Received in revised form 12 December 2009
Accepted 17 December 2009
Available online 24 December 2009

Keywords:
Hydrogen generation
Ammonia borane
Cobalt boride
Thin film
Nanoparticles
Laser ablation

ABSTRACT

Nanoparticle-assembled Co-B thin films were synthesized by Pulsed Laser Deposition (PLD) and used as catalysts for the hydrolysis of NH_3BH_3 (ammonia borane, AB) to produce molecular hydrogen. Amorphous Co-B-based catalyst powders, produced by chemical reduction of cobalt salts, were used as target material for Co-B thin film catalysts preparation through PLD. Surface morphology of Co-B powder and film catalyst was studied using Scanning Electron Microscopy (SEM) and Atomic Force Microscopy (AFM). Compositional and structural characterizations were carried out using X-photoelectron spectroscopy (XPS) and X-ray diffraction (XRD) techniques, respectively. The efficiency of both powder and film catalysts was tested by comparative kinetic analysis of the AB hydrolysis for hydrogen production. It was observed that nanoparticles produced during the laser ablation process act as active catalytic centers to produce significantly higher rate (about 6 times) of H_2 than the same amount of the corresponding Co-B powders. Almost complete conversion (95%) of AB was obtained, as confirmed by ^{11}B NMR, by using Co-B films at room temperature. Active Co-B nanoparticles on the surface of the PLD-deposited films is able to decrease the activation energy, for hydrolysis of AB, to the very low value of 34 kJ mol^{-1}. We also found that by adding small amount of $NaBH_4$ to the NH_3BH_3 solution increases the efficiency of the Co-B catalyst films, thus generating H_2 with higher rate. Maximum H_2 generation rate of about ~8.2 L H_2 min^{-1} (g of Co)$^{-1}$ and ~13 L H_2 min^{-1} (g of Co)$^{-1}$ was measured by hydrolysis of AB and mixture of (AB + $NaBH_4$) solutions, respectively.

© 2009 Elsevier B.V. All rights reserved.

1. Introduction

The search for clean fuel has become a real critical issue to overcome the problems related to emission of greenhouse gases from fossil fuels (for example petroleum) which contribute to dangerous climatic changes. Hydrogen is a definitely accepted clean fuel which when used in proton exchange membrane fuel cell (PEMFC) leads to almost zero emission of environment pollutants [1]. However, for a real clean hydrogen-based technology it is essential to develop safe and convenient hydrogen storage and on-board production systems. Although in the past considerable efforts have been focused on hydrogen storage materials, major challenges still remain [2]. Unfortunately, all the presently developed systems for hydrogen storage still lack gravimetric and/or volumetric efficiency to meet the requirement for commercial application [3].

Chemical hydrides ($NaBH_4$, $LiBH_4$, NaH, KBH_4, etc.) with high hydrogen storage in terms of gravimetric and volumetric efficiencies are the most prospective contenders to supply pure hydrogen for portable application at room temperature [4,5]. Sodium borohydride ($NaBH_4$, (SBH)) and ammonia borane (NH_3BH_3, AB) have been identified as potential candidates for on-board hydrogen production [6,7]. Among them, AB exhibits much higher hydrogen storage capacity, 19.6 wt.%, as compared to SBH, 10.8 wt.% [8]. In addition, SBH requires alkaline solution for stabilization with water while AB is highly stable and soluble in neutral water. AB can produce hydrogen by either hydrolysis or thermolysis [9] and the end product, which is nontoxic and environmentally safe, can be used to regenerate AB [10]. While thermolysis of AB requires moderate temperature, the catalytic hydrolysis can generate sustained amount of hydrogen even at room temperature.

The hydrolysis reaction rate can be effectively increased by using several inorganic and organic acids but the reaction usually becomes uncontrollable. On other hand, solid state catalysts such as precious metals (generally supported on carbon) and their salts are found to be very efficient in accelerating the hydrolysis reaction in a controllable manner. Noble catalysts like Pt, Rh, and Ru supported on Al_2O_3 [11], C [12,13] and TiO_2 [14], K_2PtCl_6 [15], and nanoclusters of Pd (0) [16], Ru (0) [17] and Rh (0) [18] have been

* Corresponding author. Tel.: +39 0461882012; fax: +39 0461881696.
E-mail address: patel@science.unitn.it (N. Patel).

0926-3373/$ – see front matter © 2009 Elsevier B.V. All rights reserved.
doi:10.1016/j.apcatb.2009.12.020

utilized in the past to enhance the hydrogen production rate. However, these catalysts do not seem to be viable for industrial application considering their cost and availability. Transition metals such as Co supported on Al_2O_3, SiO_2 and C [19], Co (0) [20,21], Ni (0) [22] and Fe (0) [23] nanoclusters, Ni based alloy [24], and Ni–SiO_2 nanospheres [25] are generally used to accelerate the hydrolysis reaction of NH_3BH_3. Cobalt boride (Co-B) is considered as a good candidate owing to its relevant catalytic activity and low cost. Co-B catalyst material can be effortlessly synthesized by simple chemical processes in which salts of this transition metal ion are reduced to elemental state by the most common reducing agents [26]. Several published papers prove that Co-B catalyst in different form can be effectively used for the hydrolysis of $NaBH_4$ [27–29]. Our previous results demonstrated that Co-B based alloy catalysts in form of Co-Cr-B [30], Co-Ni-B [31], Co-P-B [32], and Co-Ni-P-B [33] exhibit superior catalytic activity in hydrogen production by hydrolysis of SBH.

Generally, most of the previous catalysts were used as homogeneous powders which, however, have several disadvantages because (1) the separation of the catalyst from the heterogeneous mixture at the end of the reaction is difficult, (2) the catalyst particles tend to aggregate, especially when they are present at high concentrations, (3) the reaction is difficult to carry out in the presence of particulates in systems working with continuous flow. Co-B amorphous powder obtained via direct reduction of Co(II) salts by BH_4^- in aqueous solution usually display low surface area, broadly distributed particle clusters, and poor thermal stability against crystallization as a result of particle aggregation due to the exothermic nature of reduction reaction [34]. On the other hand, thin films not only have generally better catalytic properties due to their surface morphology and structure but also they can be easily recovered and reused thus being very suitable tool to act as on/off switch for generation of H_2. For all these reasons, catalysts in the form of thin films are used to solve the above mentioned powder-problems [35]. Catalytic activity is mainly a surface effect which can be enhanced by using nano-catalysts. Pulsed Laser Deposition (PLD) has emerged as viable method for the production of nanoparticles on the surface of the thin films [36]. By changing the PLD parameters, namely energy and pulse duration, the morphology and the structure of the film can be optimized for a given application. In our previous works [37,38], Co-B catalysts developed by PLD in form of nanoparticle-assembled films showed a performance similar to that of the noble metals for hydrogen production in the hydrolysis reaction of SBH.

In the present work we investigate the hydrogen production process through catalytic hydrolysis of AB using nanoparticle-assembled Co-B thin film catalyst deposited by PLD. The kinetics is studied as a function of both AB concentration and solution temperature.

2. Experimental

The detailed procedure concerning Co-B powder and film preparation is reported in our previous works [37,38]. In brief, Co-B powder catalyst, synthesized by the chemical reduction method, was used as the target for the film deposition. PLD was performed using KrF excimer laser (Lambda Physik) under vacuum condition with a base pressure of 2×10^{-5} Pa by using laser pulses of 3 J/cm^2. Details of the deposition apparatus are reported in Ref. [39]. Films were deposited on silicon substrates for the characterization and on glass substrates for checking their catalytic activity. Weight of the catalyst films was evaluated by measuring the weight of the glass slide (76 mm × 46 mm), before and after the deposition, and it was kept approximately constant for all the produced samples. The surface morphology of all catalyst powders was studied by scanning electron microscope (SEM-FEG, JSM 7001F, JEOL) equipped with energy-dispersive spectroscopy analysis (EDS, INCA PentaFET-x3) to determine the composition of the samples. Topography of the Co-B film was analyzed by Atomic Force Microscopy (AFM) using silicon as a cantilever operating in the contact mode. The relative surface area of the films was directly computed from the AFM images with a scanned area of 15 μm × 15 μm. Structural characterization of the catalyst powders was carried out by conventional X-ray diffraction (XRD) using the Cu K_α radiation (λ = 1.5414 Å) in Bragg–Brentano (θ–2θ) configuration. Studies of surface electronic states and composition of the catalysts were carried out using X-ray photoelectron spectroscopy (XPS). X-ray photoelectron spectra were acquired using a SCIENTA ESCA200 instrument equipped with a monochromatic Al K_α (1486.6 eV) X-ray source and a hemispherical analyzer. No electrical charge compensation was necessary to perform the analysis. In situ sputtering with Ar ions was performed on the film surface to remove the surface oxide (generated during the interval time elapsed from film preparation and XPS analysis) to acquire a clean spectrum. However, the quantification of the elements in the film was performed from the XPS spectra acquired before Ar sputtering. Fourier Transform Infrared Spectroscopy (FT-IR) were carried out in transmission mode at normal incidence in the spectral range between 6000 and 400 cm^{-1} using a Bruker (Equinox 55) spectrometer operated at room temperature.

^{11}B NMR spectra were acquired at 298.2 K with an Avance 400 Bruker spectrometer operating at 128.38 MHz and equipped with a 5 mm inverse broad band (BBI) probe. For each set of NMR measurements, 500 μL of AB solution was inserted into a 5 mm NMR test tube. Several aliquots were collected at different reaction times and 50 μL of D_2O was added to each sample to provide an internal lock frequency control.

For catalytic activity measurements, a solution of AB (Sigma–Aldrich) with 0.025 M was prepared. The generated hydrogen quantity was measured through a gas volumetric method in an appropriate reaction chamber with thermostatic bath, wherein the temperature was kept constant within accuracy ± 0.1 K. The chamber was equipped with pressure sensor, stirrer system, catalyst insertion device, and also coupled with an electronic precision balance to accurately measure the weight of water displaced by the hydrogen produced during the reaction course. A detailed description of the measurement apparatus is reported in Ref. [40]. In all the runs, the catalyst was placed on the insertion device (PVC circular disc with a rod) inside the reaction chamber and the system was sealed. Catalyst powder or film was added to 150 ml of the above solution, at 298 K, under continuous stirring. In order to make comparison, the stoichiometric hydrogen cumulative production yield (%) versus time was plotted instead of the hydrogen volume (ml) versus time. The efficiency of the catalyst film was compared with the corresponding powder by using analogous amount of catalyst (10 mg).

Kinetic studies of AB hydrolysis using Co-B catalysts film were carried out by varying process parameters such as the thermostatic bath temperature and the initial concentration of AB. The H_2 generation rate was measured at different temperatures to determine the activation energy involved in the catalytic hydrolysis reaction. In addition, several kinetic measurements were carried out by varying the initial concentrations of AB (from 0.025 to 0.1 M) and keeping the amount of catalyst constant, to investigate the rate dependence of the process from this parameter. In every run, a freshly prepared Co-B catalyst film was used.

In another set of experiments, a mixture of AB and SBH solution (at the total concentration of 0.025 M) was prepared where the AB/SBH molar ratio was kept constant at 9:1. The hydrolysis of this solution mixture (150 ml) was carried out using Co-B catalyst film at room temperature. The yield and the overall evolution rate of H_2 were measured and compared to those obtained for the solution

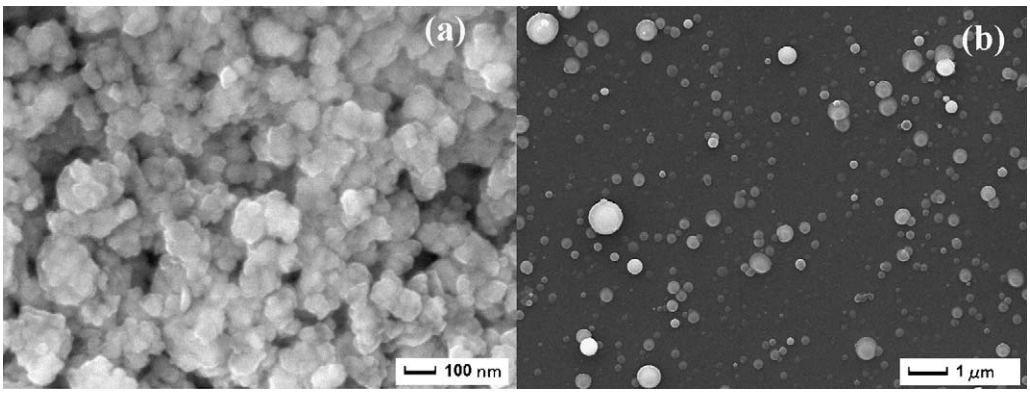

Fig. 1. SEM micrographs of Co-B catalyst: (a) powder, and (b) film deposited by PLD.

containing only AB. The hydride solution mixture was also used to explore the reusability of the Co-B catalyst film: after each catalytic activity measurement the catalyst film was recovered and retested with a newly prepared solution. Before testing, the recovered film was washed with distilled water and ethanol before drying at around 323 K under continuous N_2 flow. This step was repeated several times to establish the reusability of Co-B film catalyst.

3. Results and discussion

The SEM surface morphologies of the Co-B powder and of PLD films are reported in Fig. 1a and b, respectively. The SEM images of catalyst powder show particle-like morphology with particles having size of a few nanometers. During catalyst preparation, the use of SBH as a reducing agent causes a fast reduction of Co ions which inhibit particle growth above a few nanometers. However, these particles tend to agglomerate to minimize their high surface energy. The surface of the PLD Co-B film shows the presence of spherical particulates with a wide distribution of diameter values (average size of ~270 nm). The observed particles are generated by laser induced phase explosion process in which at higher laser fluence the irradiated target material reaches temperature of ~0.9 Tc (thermodynamic critical temperature) causing a very high homogeneous nucleation of vapor bubble. The target surface then makes a rapid transition from superheated liquid to a matrix of vapor and liquid droplets, which leave the irradiated target surface and get deposited on the substrate [41]. The size and the number density of these particles are related to the laser energy as discussed in our previous paper [37]. The 3D image (Fig. 2) obtained with AFM also confirms the rough morphology of the surface, with average RMS roughness of ~264 nm that is consistent with the particulates formation. XRD patterns (Fig. 3) of Co-B powder show a broad peak at around $2\theta = 45^\circ$ which is attributed to the amorphous state of cobalt-metalloid alloy [42]. The Co-B film does not exhibit any peak in the XRD spectra (see Fig. 3 in which only one peak related to the Si substrate is present) indicating an amorphous structure of the particles which contributes to enhance the catalytic activity. This special feature is well established in the literature and is attributed to the peculiarities of the short-range order but long-range disorder structure [43].

XPS was used to gain insight of the electronic states and surface interaction between atoms in Co-B catalyst. Fig. 4 shows the XPS spectra of $Co_{2p3/2}$ and B_{1s} electronic levels in Co-B powder and in film catalyst. For both form of catalyst, two peaks corresponding to the $Co_{2p3/2}$ level appear at the binding energies (BE) of 778.4 and 781.6 eV, indicating that Co element exists in both elemental and oxidized states. The 2+ state related to the peak of the oxidized cobalt is attributed to $Co(OH)_2$ species which, possibly, would have been formed during catalyst preparation [44] or when it was exposed to ambient atmosphere. There is no shift in the elemental BE peak of Co as compared to the standard binding energy of metallic Co. For Co-B powder, B-related XPS peaks are observed at BE values of 188.3 and 192.1 eV which corresponds to elemental and oxidized B_{1s} levels, respectively [44]. On the other hand, for Co-B film only oxidized boron species were observed with the BE of 192.5 eV. In addition, XPS spectra of O_{1s} level confirmed the existence of cobalt and boron oxide on the surface of catalyst film and powder (figure not shown). A positive shift of 1.2 eV is evident when comparing the BE of pure boron (187.1 eV) [45] to that of

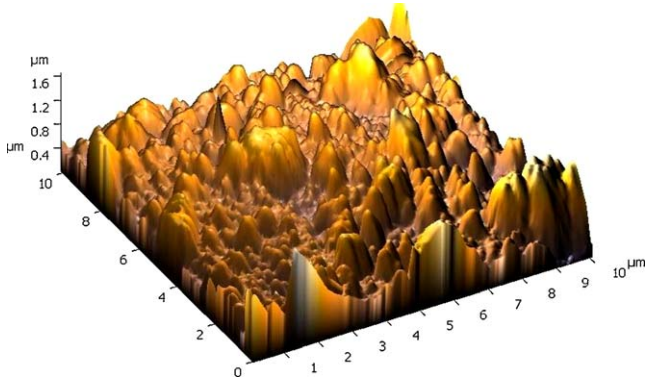

Fig. 2. 3D-AFM images of Co-B catalyst film deposited by PLD.

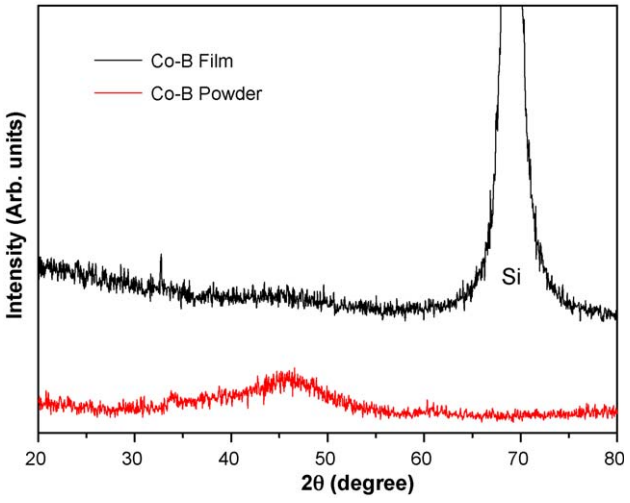

Fig. 3. XRD pattern of Co-B catalyst powder and film deposited by PLD.

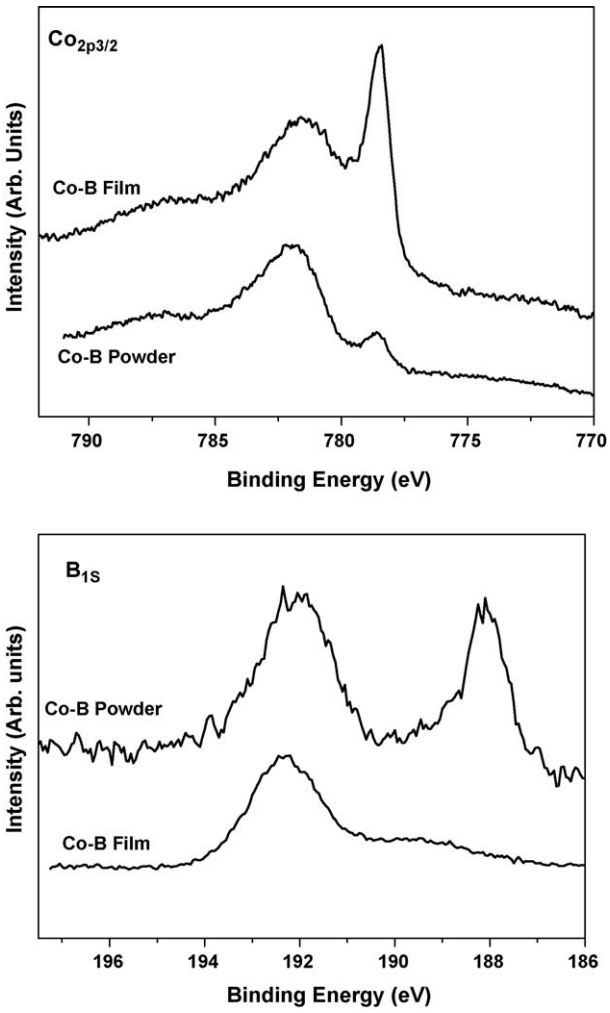

Fig. 4. XPS spectra of Co_{2p} and B_{1s} levels for Co-B catalyst powder and film deposited by PLD.

boron in the Co-B powder catalyst. This shift may suggest electron transfer from alloying B to vacant d-orbital of metallic Co: this is true for both the form of Co-B catalyst [46]. The electron-enriched metal active sites could repel the adsorption of oxygen atoms from

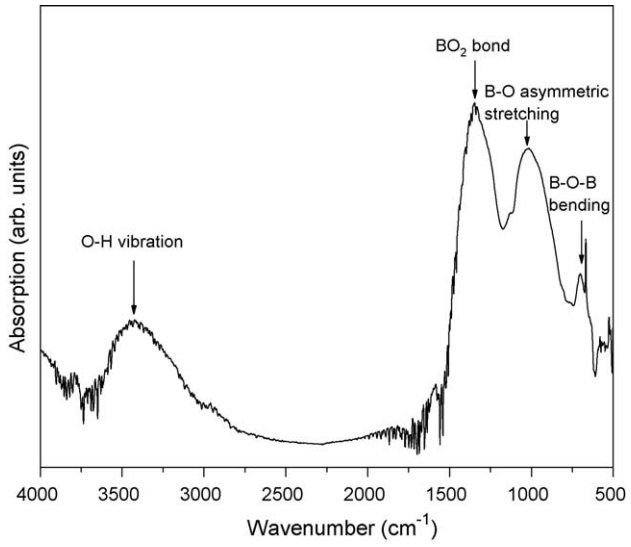

Fig. 5. FT-IR spectrum of Co-B film deposited by PLD.

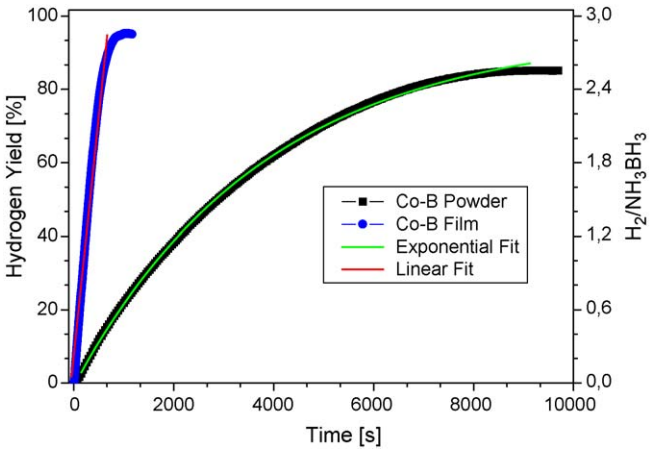

Fig. 6. Hydrogen generation yield as a function of reaction time obtained by hydrolysis of NH_3BH_3 (0.025 M) with Co-B catalyst powder and film deposited by PLD.

the ambient atmosphere, while they could be adsorbed by the electron-deficient B. In other words, alloying B could partially protect Co from oxidation in ambient condition [47]. The lack of shift in Co peak in compound catalyst is due to the heavy mass of the atom. By using the XPS spectra, the surface Co/B molar ratio on the catalyst is determined as 0.40 and 0.36 for Co-B powder and film, respectively.

B-O species in the film are also detected by FT-IR analysis showing bands at frequencies attributable to the vibration normal mode of borate BO_2^- species (Fig. 5) [48]. In addition, a broad band is observed in a frequency range of 3000–3600 cm^{-1} which is attributed to O–H vibration in $Co(OH)_2$ phase. This additional result confirms our previous finding that Co is partially oxidized and present in form of $Co(OH)_2$.

The catalytic behavior of Co-B films, synthesized by PLD, was compared with that of the corresponding Co-B powder. Hydrogen generation yield was measured, as a function of time, during the hydrolysis of AB solution (0.025 M) in presence of Co-B powder and of PLD film at 298 K (Fig. 6). The figure clearly shows that both the Co-B catalysts are active and produce hydrogen instantaneously as soon as they come in contact with the AB solution. However, the Co-B film exhibits much higher catalytic activity as compared to the Co-B powder and it was able to complete the reaction within 15 min while the same amount of Co-B powder catalyst (~10 mg) took about 145 min. The total amount of hydrogen generated by hydrolysis of AB using Co-B film (H_2/NH_3BH_3 = 2.85) is closer to the expected quantitative yield, from the reaction stoichiometry (H_2/NH_3BH_3 = 3.0) than that generated by Co-B powder (H_2/NH_3BH_3 = 2.55). In addition to the volumetric measurement of H_2 generation, the conversion of the AB was also monitored through ^{11}B NMR by comparing the intensity of the AB signal in the NMR spectra during the course of the reaction. The intensity of ^{11}B peak of AB at −23.9 ppm slowly decreases as the reaction proceeds due to hydrogen evolution. After completion of the reaction, the NMR peak due to AB entirely disappears whereas a broad peak at +11.6 ppm attributed to borate (BO_2^-) species is visible in the spectra (Fig. 7). Thus the above result indicates that the hydrolysis reaction of NH_3BH_3 over Co-B film catalyst proceeds by evolution of nearly 3 moles of H_2, leaving NH_4^+ and BO_2^- as end products, in agreement with recent literature reports [11,12].

Several films synthesized by using the same PLD parameters showed almost identical (±5%) H_2 generation rate, thus establishing the reproducibility of our produced PLD films. During the reaction, the catalyst films were quite stable in terms of hydrogen production.

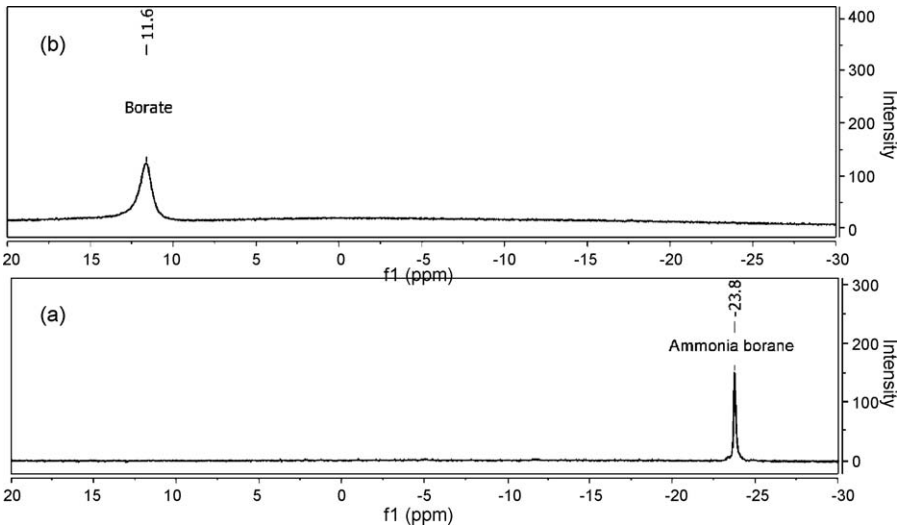

Fig. 7. ^{11}B-proton decoupled NMR spectra of: (a) freshly prepared aqueous NH_3BH_3 solution, and (b) reaction product after hydrolysis of NH_3BH_3.

The H_2 generation yield values for Co-B powder reported in Fig. 6 was perfectly fitted by using a single exponential function as described in Ref. [32],

$$[H_2](t) = [H_2]_{max} \times (1 - e^{-k_1 t}) = 3[[AB]_0 \times (1 - e^{-k_1 t})] \quad (1)$$

where $[AB]_0$ is the initial concentration of AB in the solution and k_1 is the overall rate constant. This suggests that hydrolysis reaction catalyzed by Co-B powder is a first order process with respect to AB. Importantly, linear fitting of the H_2 generation data produced with Co-B film show a zero order dependence from AB concentration as it will be further discussed in greater details below.

A numerical procedure, described elsewhere [38], was utilized to obtain the maximum value of the hydrogen generation rate (R_{max}) for both the catalysts. The maximum H_2 generation rate obtained for the same amount of catalyst (10 mg) by using the Co-B films (~2420 ml/min/g catalyst) has been found about 6 times higher than that obtained using the Co-B powder (~400 ml/min/g catalyst). This better catalytic performance is mainly attributed to surface morphology effects in nanoparticle-assembled films (Figs. 1 and 2). The nanoparticles, having average size of around 300 nm, are the highly active sites for the hydrolysis reaction even at low AB concentration and at room temperature. These active Co-B nanoparticles promote the hydrogen production immediately after coming in contact with the solution, as seen by the high initial H_2 generation rate (Fig. 6). The relative surface area calculated on the basis of the AFM image of the nanoparticle-assembled Co-B film shows 70–75% increment, with respect to the flat surface (details of the calculation procedure are reported in Ref. [38]). Thus, the Co-B particulates, produced by PLD on the film surface, increases the effective surface area while acting as efficient site to enhance the catalytic activity. However, we suspect that additional features of the Co-B particles could be relevant to justify the efficiency of the catalyst. We are making indeed new investigations to try to improve our understanding of the PLD particles.

In order to study the effect of AB concentration on hydrogen generation rate we preformed a set of experiments with different initial concentrations of AB while keeping the amount of Co-B catalyst nearly constant in the film. Fig. 8 presents the plot of hydrogen generated volume, as a function of time, obtained from hydrolysis of AB solution by using 4 different AB initial concentrations (0.025, 0.05, 0.075, and 0.10 M). A slight increase in the hydrogen generation rate was observed when using the highest initial concentration of AB. However, as shown in the inset of Fig. 8, the logarithmic dependence of R_{max} from AB concentration can be fitted with a straight line having a slope of 0.17. The near-zero value of the slope indicates the zero order kinetics of the reaction with respect to the AB concentration for the Co-B film catalyst, thus confirming our previous findings. The high effective surface area, provided by the catalytic active nanoparticles, is able to confine the hydrogen generation to a surface reaction. On the contrary, the first order kinetics involving diffusion of BH_3^- on the catalyst surface [32] is the rate limiting step in the case of Co-B powder. Similar zero order kinetics with respect to AB concentration was proposed by Xu and Chandra [19] (Co/γ-Al_2O_3), Yao et al. [24] (NiAg alloy catalyst), and Özkar et al. [16] (Ru and Pd nanoclusters).

The H_2 generation yield as a function of time was measured at different solution temperatures by hydrolysis of AB (0.025 M) solution using Co-B powder and film catalysts as reported in Figs. 9 and 10, respectively. The Arrhenius plot of the hydrogen production rate (inset of Figs. 9 and 10) gives an activation energy value of 34 ± 1 kJ mol^{-1} for Co-B film which is lower than

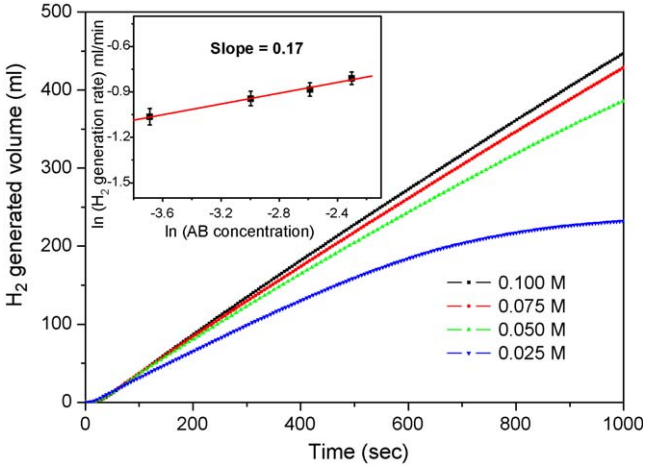

Fig. 8. Hydrogen generated volume as a function of reaction time, with Co-B catalyst film, obtained by hydrolysis of NH_3BH_3 solution with 4 different concentrations of NH_3BH_3 ranging from 0.025 to 0.10 M. Inset shows the plot of ln(H_2 generation rate) vs ln(concentration of NH_3BH_3) to determine the reaction order with respect to NH_3BH_3.

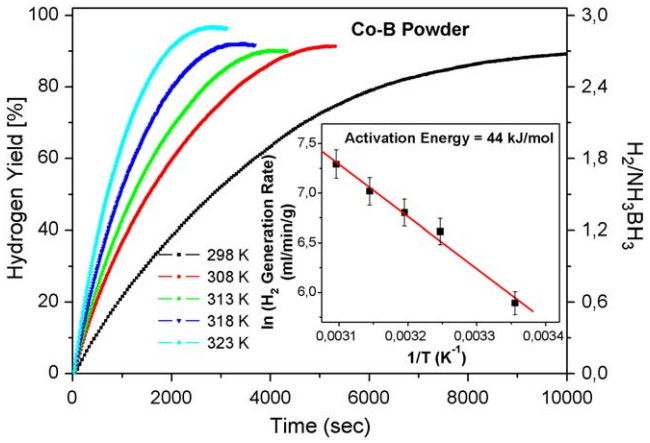

Fig. 9. Hydrogen generation yield as a function of reaction time by hydrolysis of NH_3BH_3 (0.025 M) solution with Co-B catalyst powder, measured at 5 different solution temperatures. Inset shows the Arrhenius plot of the H_2 generation rates.

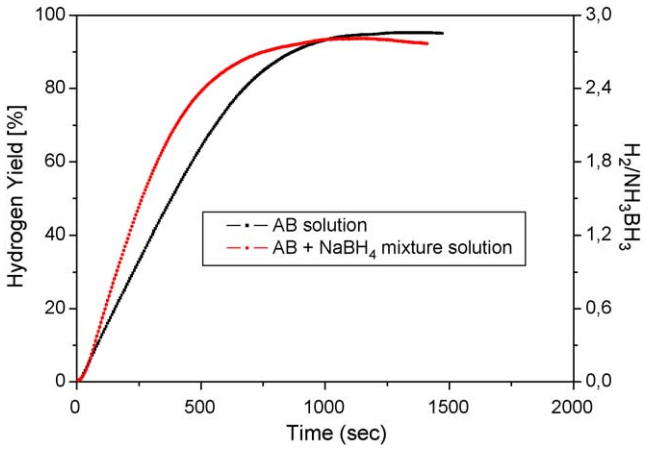

Fig. 11. Hydrogen generation yield as a function of reaction time by hydrolysis of NH_3BH_3 (0.025 M) solution and mixture of NH_3BH_3 + $NaBH_4$ solution (0.025 M) (molar ratio of NH_3BH_3:$NaBH_4$ is kept at 9:1) with Co-B catalyst film deposited by PLD.

that obtained with Co-B powder (44 ± 1 kJ mol^{-1}). This value is also much lower than that reported in the literature for noble metal catalysts like Ru (47 kJ mol^{-1}) [17] and Rh (67 kJ mol^{-1}) nanoclusters [18], Pd metal (44 kJ mol^{-1}) [16], Ru/C (76 kJ mol^{-1}) [13], and K_2PtCl_6 (86 kJ mol^{-1}) [15]. The activation energy value obtained in the present case is also lower than that obtained by other catalysts such as NiAg (51.5 kJ mol^{-1}) [24], Co/γ-Al_2O_3 (62 kJ mol^{-1}) [19], Co-Mo-B/Ni foam (44 kJ mol^{-1}) [49], and Co (0) nanoclusters (46 kJ mol^{-1}) [20].

Recently, Umegaki et al. [22,25] demonstrated that Ni is able to generate H_2 from the hydrolysis of SBH and AB mixture at higher rate than from solutions containing only the AB species. The authors proved that SBH is able to activate the catalyst surface thus enhancing the overall rate. In order to understand if such a behavior could also observed in our Co-B catalyst film, we measured the H_2 generation yield (Fig. 11), as a function of time, through hydrolysis of AB and SBH mixture with the molar ratio [AB]/[$NaBH_4$] = 9. Indeed, the enhancing catalytic effect of the small amount of SBH present into AB solution was clearly visible since we observed an increment of about 60% in the R_{max} value as measured by hydrolysis of the hydride mixture (3500 ml/min/g catalyst) as compared to that of pure AB solution (2200 ml/min/g catalyst). As confirmed by XPS analysis, in present Co-B catalyst film there is a partial oxidation of Co on the surface. This oxide is in form of cobalt hydroxide ($Co(OH)_2$) which can be easily reduced by SBH in the course of the hydrolysis thus explaining the enhanced catalytic effect. Liu and Li [50] showed experimentally that $Co(OH)_2$ intermediate can acts as nuclei for the precipitation of Co-B active phase during the reaction with $NaBH_4$.

Reusability and durability of the catalyst are other important factors to be considered before moving towards applications. A specific experiment was performed to recycle the sample many times though the following steps: (1) carrying out the hydrolysis reaction with a freshly prepared catalyst film; (2) recollecting the catalyst film; (3) washing catalyst film with distilled water and ethanol before drying at around 323 K under continuous N_2 flow; (4) reusing this catalyst with a newly prepared solution (AB + SBH). The hydrogen generation yield as a function of time, for a given number of runs, as obtained by hydrolysis of AB and SBH mixture solution ([AB] + [$NaBH_4$] = 0.025 M, [AB]/[$NaBH_4$] = 9) is reported in Fig. 12. It is clearly observed that after every cycle the catalytic activity of the Co-B catalyst film decreases and takes longer time to complete the reaction. Indeed, there is a significant decrease in H_2 generation rate from 1st cycle to 5th cycle; this decrease could be due to the detachment of few weakly bounded nanoparticles from the catalyst film surface during the vigorous stirring procedure in the reacting system. We have actually observed a significant loss of catalyst weight after each reaction cycle and after fifth cycle only small amount of film was visible. The total number of H_2 moles

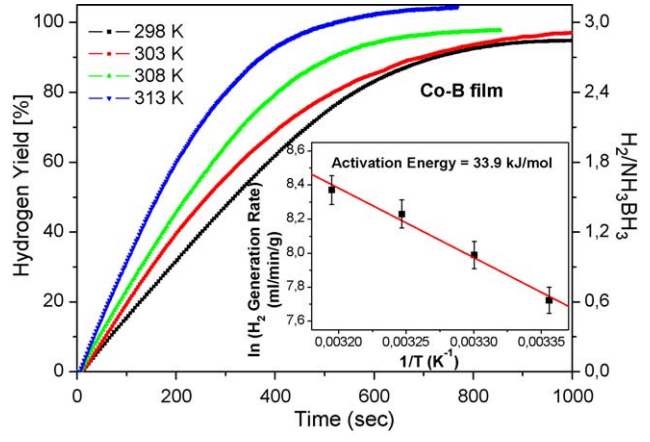

Fig. 10. Hydrogen generation yield as a function of reaction time by hydrolysis of NH_3BH_3 (0.025 M) solution with Co-B catalyst film deposited by PLD, measured at 4 different solution temperatures. Inset shows the Arrhenius plot of the H_2 generation rates.

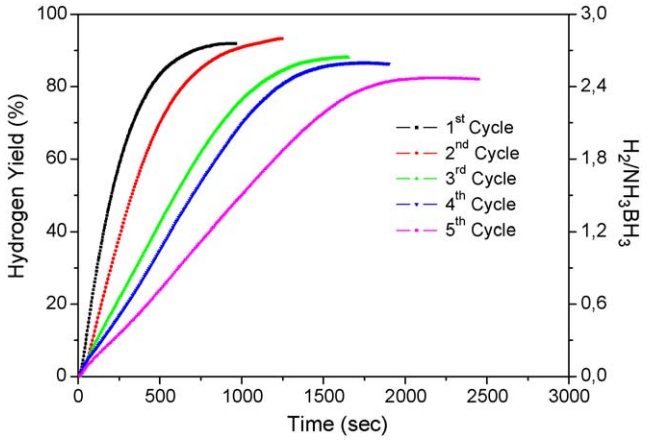

Fig. 12. Cycling of Co-B catalyst film for hydrogen generation yield as a function of reaction time for hydrolysis of NH_3BH_3 + $NaBH_4$ solution mixture (0.025 M) (molar ratio of NH_3BH_3:$NaBH_4$ is kept at 9:1).

generated during the reaction also decreases by small amount from 2.85 (1st cycle) to 2.5 (5th cycle). This proves that our nanoparticle-assembled Co-B thin film catalyst can be reused but with reduced efficiency. Specific studies are under way to improve the adhesion of the film with the substrate and to investigate the catalyst surface at the end of the reaction in order to improve the catalyst durability.

Finally, we compare the H_2 generation rates obtained with the present nanoparticle-assembled Co-B catalyst film with those reported in the literature for different solid catalysts. Generally most of these reports indicate the H_2 generation rate per gram of the active metal catalyst (i.e. ml/min g of metal catalyst). In our case, only Co is the active metal catalyst and, therefore, the H_2 generation rate as calculated after linear fitting of our data is ~8200 ml H_2 min^{-1} (g of Co)$^{-1}$ or ~13,000 ml H_2 min^{-1} (g of Co)$^{-1}$ for hydrolysis of AB or mixture of (AB + SBH) solutions, respectively. The Co content was obtained by the XPS data of the film catalyst (Co/B molar ratio = 0.36). The H_2 generation rate value obtained in the present case is far better than those found for cobalt based catalyst such as Co/C (~2000 ml H_2 min^{-1} (g of Co)$^{-1}$) [19], PVP stabilized Co(0) nanoclusters (~1500 ml H_2 min^{-1} (g of Co)$^{-1}$) [20] and Co-Al_2O_3 (~630 ml H_2 min^{-1} (g of Co)$^{-1}$) [13] catalyst. Our rate value is also higher than those achieved with PVP stabilized Ni (~1100 ml H_2 min^{-1} (g of Ni)$^{-1}$) [22] and Fe nanoparticles (~1000 ml H_2 min^{-1} (g of Fe)$^{-1}$) [23] catalyst. The H_2 generation rate of 8500 ml H_2 min^{-1} (g of Pt)$^{-1}$ was reported for noble metal like Pt/Al_2O_3 [11,18], a value which is very similar to our film catalyst. Recently, Zahmakiran and Özkar [18] and Durap et al. [17] reported on high H_2 generation rate for hydrolysis of AB by using Rh(0) (~20,000 ml H_2 min^{-1} (g of Rh)$^{-1}$) and Ru(0) nanclusters (~16,700 ml H_2 min^{-1} (g of Ru)$^{-1}$). These values are higher than that observed with our Co-B catalyst films. However, we have to note that Pt, Ru and Rh are the costliest materials and not preferable for the hydrogen economy.

To conclude, PLD is able to produce nanoparticle-assembled films with non-noble metal, like cobalt, having catalytic efficiency comparable to that of costliest metals like Pt and Ru. The other main advantage of our catalyst film is that it can be recovered easily and hence it can be used as ON/OFF switch for H_2 generation: this switching property is very difficult to achieve with powder catalysts.

4. Conclusions

We have proved that nanoparticle-assembled Co-B thin films, synthesized by PLD, act as really efficient catalysts for hydrolysis of AB to produce hydrogen. The comparison was made with same amount of Co-B powders which indeed exhibit a lower rate (about 6 times) of H_2 generation. Almost complete conversion of AB was obtained, as confirmed by ^{11}B NMR, with Co-B films at room temperature: 2.85 moles of H_2 have been generated instead of the maximum expected, i.e. 3.0 equivalents. The activation energy of the rate limiting process involved in the final hydrogen production is as low as 34 kJ mol^{-1} and the H_2 generation rate is similar to that reported in the literature for noble metal like Pt/Al_2O_3. The peculiarities of the Co-B nanoparticles, produced by PLD, are related to their well established spherical form and to their density distribution which is preserved against coalescence, a deleterious process inhibiting the favorable surface/volume ratio that is basic to the catalysis process. In presence of the Co-B film catalyst, the order of the reaction with respect to the AB concentration is zero, a kinetics feature related to the morphological properties of the nanoparticles that are able to confine the hydrogen generation to a surface reaction. On the contrary, the first order kinetics, involving diffusion of BH_4^- on the catalyst surface, is the rate limiting step in the case of Co-B powder. Nanoparticle-assembled Co-B thin film catalyst can be reused but with reduced efficiency because, currently, we are coping with adhesion failures that we intend to eliminate in the forthcoming experiments. Finally we found that adding a small amount of SBH to the AB solution, the efficiency of the Co-B catalyst films increases thus generating H_2 with higher rate. The role of SBH is to activate the catalyst by reducing oxidized forms of Cobalt ($Co(OH)_2$) as observed by XPS and FT-IR analysis.

Acknowledgements

We thank N. Bazzanella for SEM-EDS analysis, C. Armellini for XRD analysis, and S. Torrengo for XPS analysis. The research activity is financially supported by the Hydrogen-FISR Italian project.

References

[1] A.L. Dicks, J. Power Sources 61 (1996) 113.
[2] L. Schlapbach, A. Züttel, Nature 414 (2001) 353.
[3] L. Zhou, Renew. Sustain. Energy Rev. 9 (2005) 395.
[4] S.C. Amendola, S.L. Sharp-Goldman, M.S. Janjua, N.C. Spencer, M.T. Kelly, P.J. Petillo, M. Binder, Int. J. Hydrogen Energy 25 (2000) 969.
[5] R.B. Biniwale, S. Rayalu, S. Devotta, M. Ichikawa, Int. J. Hydrogen Energy 33 (2008) 360.
[6] T. Umegaki, J.M. Yan, X.B. Zhang, H. Shioyama, N. Kuriyama, Q. Xu, Int. J. Hydrogen Energy 34 (2009) 2303.
[7] F.H. Stephens, V. Pons, R.T. Baker, Dalton Trans. 25 (2007) 2613.
[8] B. Peng, J. Chen, Energy Environ. Sci. 5 (2008) 479.
[9] M. Diwan, V. Diakov, E. Shafirovich, A. Varma, Int. J. Hydrogen Energy 33 (2008) 1135.
[10] S. Hausdorf, F. Baitalow, G. Wolf, F.O.R.L. Mertens, Int. J. Hydrogen Energy 33 (2008) 608.
[11] Q. Xu, M. Chandra, J. Alloys Compd. 446 (2007) 729.
[12] M. Chandra, Q. Xu, J. Power Sources 156 (2006) 190.
[13] S. Basu, A. Brockman, P. Gagare, Y. Zheng, P.V. Ramachandran, W.N. Delgass, J.P. Gore, J. Power Sources 188 (2009) 238.
[14] V.I. Simagina, P.A. Storozhenko, O.V. Netskina, O.V. Komova, G.V. Odegova, Y.V. Larichev, A.V. Ishchenko, A.M. Ozerova, Catal. Today 138 (2008) 253.
[15] N. Mohajeri, A. T-Raissi, O. Adebiyi, J. Power Sources 167 (2007) 482.
[16] Ö. Metin, S. Sahin, S. Özkar, Int. J. Hydrogen Energy 34 (2009) 6304.
[17] F. Durap, M. Zahmakiran, S. Özkar, Int. J. Hydrogen Energy 34 (2009) 7223.
[18] M. Zahmakiran, S. Özkar, Appl. Catal. B: Environ. 89 (2009) 104.
[19] Q. Xu, M. Chandra, J. Power Sources 163 (2006) 364.
[20] Ö. Metin, S. Özkar, Energy Fuel 23 (2009) 3517.
[21] T.J. Clark, G.R. Whittell, I. Manners, Inorg. Chem. 46 (2007) 7522.
[22] T. Umegaki, J.M. Yan, X.B. Zhang, H. Shioyama, N. Kuriyama, Q. Xu, Int. J. Hydrogen Energy 34 (2009) 3816.
[23] J.M. Yan, X.B. Zhang, S. Han, H. Shioyama, Q. Xu, Angew. Chem. Int. Ed. 47 (2008) 2287.
[24] C.F. Yao, L. Zhuang, Y.L. Cao, X.P. Ai, H.X. Yang, Int. J. Hydrogen Energy 33 (2008) 2462.
[25] T. Umegaki, J.M. Yan, X.B. Zhang, H. Shioyama, N. Kuriyama, Q. Xu, J. Power Sources 191 (2009) 209.
[26] S.U. Jeong, E.A. Cho, S.W. Nam, I.H. Oh, U.H. Jung, S.H. Kim, Int. J. Hydrogen Energy 32 (2007) 1749.
[27] J. Zhao, H. Ma, J. Chen, Int. J. Hydrogen Energy 32 (2007) 4711.
[28] W. Ye, H. Zhang, D. Xu, L. Ma, B. Yi, J. Power Sources 164 (2007) 544.
[29] P. Krishnan, S. Advani, A.K. Prasad, Appl. Catal. B 86 (2009) 137.
[30] R. Fernandes, N. Patel, A. Miotello, Appl. Catal. B: Environ. 92 (2009) 68.
[31] R. Fernandes, N. Patel, A. Miotello, M. Filippi, J. Mol. Catal. A: Chem. 298 (2009) 1.
[32] N. Patel, R. Fernandes, A. Miotello, J. Power Sources 188 (2009) 411.
[33] R. Fernandes, N. Patel, A. Miotello, Int. J. Hydrogen Energy 34 (2009) 2893.
[34] Z.B. Yu, M.H. Qiao, H.X. Li, J.F. Deng, Appl. Catal. A 163 (1997) 1.
[35] I. Sopyan, M. Watanabe, S. Murasawa, K. Hashimoto, A. Fujishima, J. Photochem. Photobiol. A: Chem. 98 (1996) 79.
[36] A. Miotello, R. Kelly, Appl. Phys. Lett. 67 (1995) 3535.
[37] N. Patel, G. Guella, A. Kale, A. Miotello, B. Patton, C. Zanchetta, L. Mirenghi, P. Rotolo, Appl. Catal. A: Gen. 323 (2007) 18.
[38] N. Patel, R. Fernandes, G. Guella, A. Kale, A. Miotello, B. Patton, C. Zanchetta, J. Phys. Chem. C 112 (2008) 6968.
[39] M. Bonelli, C. Cestari, A. Miotello, Meas. Sci. Technol. 10 (1999) N27.
[40] C. Zanchetta, B. Patton, G. Guella, A. Miotello, Meas. Sci. Technol. 18 (2007) N21.
[41] A. Miotello, R. Kelly, Appl. Phys. A: Mater. Sci. Process 69 (1999) S67.
[42] G.W. Pei, W.L. Zhong, S.B. Yue, Univ. Press. Jinan (1989) 453.
[43] A. Baiker, Faraday Discuss. Chem. Soc. 87 (1989) 239.
[44] W.L. Dai, M.H. Qiao, J.F. Deng, Appl. Surf. Sci. 120 (1997) 119.
[45] H. Li, H.X. Li, W.L. Dai, Z. Fang, J.F. Deng, Appl. Surf. Sci. 152 (1999) 25.
[46] H. Li, W. Wang, H. Li, J.F. Deng, J. Catal. 194 (2000) 211.
[47] H. Li, Y. Wu, H. Luo, M. Wang, Y. Xu, J. Catal. 214 (2003) 15.
[48] A.N. Kale, A. Miotello, P. Mosaner, Appl. Surf. Sci. 252 (2006) 7904.
[49] H.B. Dai, L.L. Gao, Y. Liang, X.D. Kang, P. Wang, J. Power Sources 195 (2010) 307.
[50] B.H. Liu, Q. Li, Int. J. Hydrogen Energy 33 (2009) 7385.